

MICRO-SCALE HEAT TRANSFER. ALGORITHM BASING ON THE CONTROL VOLUME METHOD AND THE IDENTIFICATION OF RELAXATION AND THERMALIZATION TIMES USING THE SEARCH METHOD

BOHDAN MOCHNACKI^{1*}, MARIUSZ CIESIELSKI²

¹*Higher School of Labour Safety Management in Katowice, 40-007 Katowice, Bankowa 8, Poland*

²*Częstochowa University of Technology, Institute of Computer and Information Sciences,
42-201 Częstochowa, Dabrowskiego 69, Poland*

*Corresponding author: bohdan.mochnacki@im.pcz.pl

Abstract

The thermal processes proceeding in micro-domains can be described, among others, using the dual phase lag model (DPLM). According to the newest opinions the DPLM constitutes a very good description of the real heat transfer processes proceeding in the micro-scale, in particular on account of extremely short duration, extreme temperature gradients and the very small geometrical dimensions of domain considered. The base of DPLM formulation is a generalized form of Fourier law in which two times τ_q , τ_T appear (the relaxation time and thermalization one, respectively). The numerical solution of the problem discussed bases on the author's version of the Control Volume Method adapted to resolve the hyperbolic partial differential equations. The example illustrating the method application concerns the estimation of τ_q and τ_T using the algorithm basing on the search method and the thin metal film subjected to the laser pulse is considered.

Key words: micro-scale heat transfer, Control Volume Method, external heating, numerical simulation, estimation of lag times

1. INTRODUCTION

The classical form of the Fourier equation bases on the assumption of infinite velocity of heat propagation and in the case of the macro models this assumption is fully acceptable. The other approach should be used in the case of micro-scale heat transfer modeling. It results, first of all, because of extremely short duration, extreme temperature gradients and very small geometrical dimensions of the domain considered and then the generalized form of the Fourier law should be taken into account. The generalized forms of the Fourier law result from the introduction of heat flux lag time (with respect to temperature gradient) called the relaxation time or

two lag times concerning both the heat flux and the temperature gradient (the relaxation and thermalization times). The first generalization leads to the governing equation called the Cattaneo-Vernotte equation (Cattaneo, 1958), while the second generalization to the dual phase lag model (DPLM) (Chen et al., 2004; Zhang, 2007; Tzou, 1995; Majchrzak et al., 2009a, 2009b). This equation contains a second order time derivative and higher order mixed derivative in both time and space and constitutes a basis of considerations presented in this paper. Additionally, the boundary conditions supplementing the basic equation should be adequately reconstructed.

To obtain the effective solution of the dual phase lag equation the numerical methods must be used. In this paper the control volume method is proposed.

According to the opinion of many experts the CVM constitutes the very convenient tool for solving the various problems from the scope of heat transfer. The classical version of CVM (macroscale heat conduction) concerns the steady and transient problems proceeding in the domain which is divided into control volumes of the regular shape (e.g. rectangles or cuboids (Szargut, 1977)). The authors of this paper proposed the generalization of CVM (2D problems) consisting in the introduction of control volumes corresponding to the Voronoi polygons (Ciesielski & Mochnacki, 2014a, 2014b). The method has been also successfully used for numerical modeling of solidification process both for the macro models (Mochnacki & Ciesielski, 2007a; Domanski et al., 2010) and micro/macro ones (Mochnacki & Ciesielski, 2007b). Below, the authors present the numerical algorithm basing of the control volume method for the case of microscale heat transfer problems described by DPL equation.

The numerical algorithm and computer program worked out within this work is used for the solution of the inverse problem concerning the identification of relaxation and thermalization times appearing in the DPL equation (e.g., Majchrzak & Mochnacki, 2014; Mochnacki & Paruch, 2013). The search method of the inverse problem solution used here consists in the division of the possible ranges of times τ_q and τ_T into sub-intervals, next for each pair $(\tau_q)_i$ and $(\tau_T)_j$ the direct task is solved. The quality of the solution obtained results from the value of functional J corresponding to least squares criterion. The optimal values of $(\tau_q)_i$ and $(\tau_T)_j$ arise from the minimal value of J . The method proposed is very simple, but allows one, among others, to observe the shape of J and to check that its minimum appears only at the one point.

2. GOVERNING EQUATIONS

Let us consider the well-known diffusion equation

$$c \frac{\partial T(X, t)}{\partial t} = -\nabla \cdot \mathbf{q}(X, t) + Q(X, t) \quad (1)$$

where c is a volumetric specific heat, $\mathbf{q}(X, t)$ is a heat flux vector, $Q(X, t)$ is a capacity of internal heat sources, X, t are the geometrical co-ordinates and time.

Assuming that the value of heat flux is determined by the Fourier law

$$\mathbf{q}(X, t) = -\lambda \nabla T(X, t) \quad (2)$$

where λ is a thermal conductivity of the material, $\nabla T(X, t)$ is a temperature gradient, one finally obtains the energy equation in the form

$$c \frac{\partial T(X, t)}{\partial t} = \nabla \cdot [\lambda \nabla T(X, t)] + Q(X, t) \quad (3)$$

The equation (3) is widely and successfully applied in engineering heat conduction problems, in which the system has a large dimension ($\geq 10^{-3}$ m) and the duration of the process is relatively long ($\geq 10^{-3}$ s) (Chen et al., 2004; Zhang, 2007).

To take into account the finite value of the thermal wave propagation (which can be essential in the case of microscale heat transfer modeling) the modifications of the Fourier law have been introduced. The first of them takes into account a lag between the heat flux vector and the temperature gradient

$$\mathbf{q}(X, t + \tau_q) = -\lambda \nabla T(X, t) \quad (4)$$

where τ_q is called the relaxation time and this assumption leads to the modified energy equation called the Cattaneo-Vernotte one (Cattaneo, 1958).

The next generalization of the Fourier law has been presented by Tzou (1995), in particular

$$\mathbf{q}(X, t + \tau_q) = -\lambda \nabla T(X, t + \tau_T) \quad (5)$$

where τ_q is, as previously, a relaxation time, while τ_T is a thermalization time.

Using the Taylor series expansions, the following first-order approximation of equation (5) is obtained

$$\begin{aligned} \mathbf{q}(X, t) + \tau_q \frac{\partial \mathbf{q}(X, t)}{\partial t} = \\ -\lambda \left[\nabla T(X, t) + \tau_T \frac{\partial \nabla T(X, t)}{\partial t} \right] \end{aligned} \quad (6)$$

Introducing this formula to the equation (1) one has (Chen et al., 2004; Zhang, 2007; Tzou, 1995; Majchrzak et al., 2009a, 2009b)

$$\begin{aligned} X \in \Omega: \quad c \left[\frac{\partial T(X, t)}{\partial t} + \tau_q \frac{\partial^2 T(X, t)}{\partial t^2} \right] = \\ \nabla \cdot [\lambda \nabla T(X, t)] + \tau_T \frac{\partial \nabla \cdot [\lambda \nabla T(X, t)]}{\partial t} \\ + Q(X, t) + \tau_q \frac{\partial Q(X, t)}{\partial t} \end{aligned} \quad (7)$$



Below, the axially-symmetrical task is discussed $X = \{r, z\}$ and then the component $\nabla \cdot [\lambda \nabla T(r, z, t)]$ corresponds to

$$\nabla \cdot [\lambda \nabla T(r, z, t)] = \frac{1}{r} \frac{\partial}{\partial r} \left[r \lambda \frac{\partial T(r, z, t)}{\partial r} \right] + \frac{\partial}{\partial z} \left[\lambda \frac{\partial T(r, z, t)}{\partial z} \right] \quad (8)$$

The domain considered is limited by the planes $z = 0, z = Z$ and surface $r = R$ (figure 1).

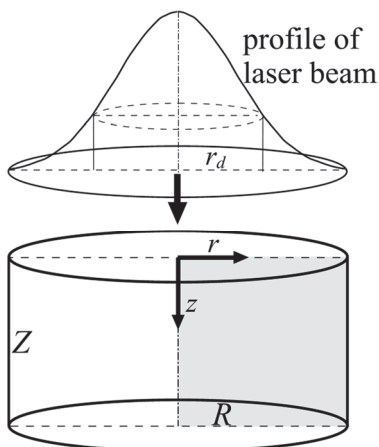


Fig. 1. Cylindrical micro-domain

Under femtosecond laser irradiation on the upper surface limiting the system, the energy is delivered into the metal and their absorption occurs. The internal heat source $Q(r, z, t)$ generated inside of metal is connected with the laser action (Chen & Beraun, 2001)

$$Q(r, z, t) = \sqrt{\frac{\beta}{\pi}} \frac{1-R_f}{t_p \delta} I_0 \exp\left(-\frac{z}{\delta}\right) \exp\left(-\frac{r^2}{r_d^2}\right) \left| \exp\left(-\beta \left(\frac{t-2t_p}{t_p}\right)^2\right) \right| = I_r(r) I_z(z) I_t(t) \quad (9)$$

where

$$I_r(r) = \exp\left(-\frac{r^2}{r_d^2}\right), \quad I_z(z) = I_0 \frac{1-R_f}{\delta} \exp\left(-\frac{z}{\delta}\right), \\ I_t(t) = \frac{\sqrt{\beta}}{t_p \sqrt{\pi}} \exp\left(-\beta \left(\frac{t-2t_p}{t_p}\right)^2\right) \quad (10)$$

and r_d is the characteristic radius of laser beam (r_d determines the circular boundary that contains 63% of the total beam power acting on the metal surface), I_0 is the laser intensity, R_f is the reflectivity of the irradiated surface, δ is the optical penetration depth, and $\beta = 4\ln 2$ and t_p is the characteristic time of laser pulse.

The action of laser beam is taken into account by the internal heat source $Q(r, z, t)$ introduction, while the dimensions Z and R are large enough that on the appropriate boundaries the adiabatic conditions can be assumed. So

$$(r, z) \in \Gamma_\infty : q_b(r, z, t) = 0. \quad (11)$$

It should be pointed out that the DPLM requires the transformation of boundary conditions which appear in the typical macro heat conduction models

$$(r, z) \in \Gamma : q_b(r, z, t) + \tau_q \frac{\partial q_b(r, z, t)}{\partial t} = -\lambda \left[\mathbf{n} \cdot \nabla T(r, z, t) + \tau_T \frac{\partial [\mathbf{n} \cdot \nabla T(r, z, t)]}{\partial t} \right] \quad (12)$$

and in the case considered one has

$$(r, z) \in \Gamma : -\lambda \left[\mathbf{n} \cdot \nabla T(r, z, t) + \tau_T \frac{\partial [\mathbf{n} \cdot \nabla T(r, z, t)]}{\partial t} \right] = 0 \quad (13)$$

The initial conditions (the initial temperature of domain and the initial heating rate) are also given

$$t = 0 : T(r, z, 0) = T_0, \quad \left. \frac{\partial T(r, z, t)}{\partial t} \right|_{t=0} = 0 \quad (14)$$

where T_0 is the constant initial temperature.

3. CONTROL VOLUME METHOD

At the stage of numerical computations the control volume method (CVM) is used. The choice of the method is not accidental, because the CVM constitutes a very effective tool for numerical modeling of heat transfer processes. To our knowledge, the method has not been used so far for numerical simulation of microscale heat transfer problems basing on the DPL equation.

At the beginning of the method application the domain considered is divided into small cells (con-



trol volumes) – in the case discussed the shape of control volumes is regular one (the rings of rectangular section), but the more complex discretization (e.g. the Voronoi polygons) can be also taken into account (Ciesielski & Mochnacki, 2014a, 2014b). The solution of transient problems requires the time grid introduction, too.

The CVM algorithm allows one to find the transient temperature field at the set of nodes corresponding to the central points of control volumes. The thermal capacities are concentrated at the nodes representing elements, while the thermal resistances are concentrated on the sectors joining the nodes.

The nodal temperatures can be found on the basis of energy balances for the successive volumes. The energy balances corresponding to heat exchange between the analyzed control volume and adjoining control volumes results from the integration of energy equation with respect to volume and time. In figure 2 the domain discretization, while in figure 3 the selected internal and boundary control volumes are shown.

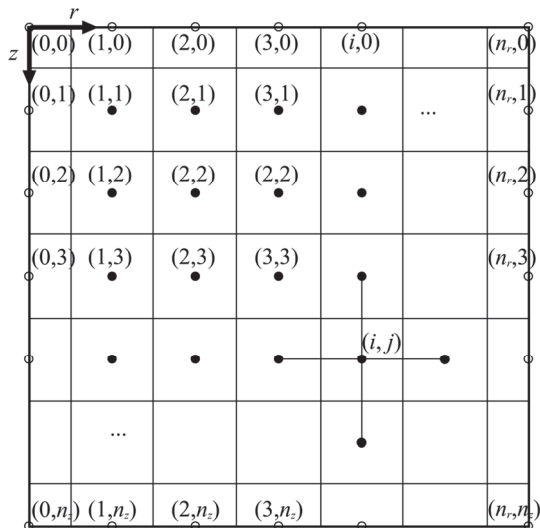


Fig. 2. The discretization of domain

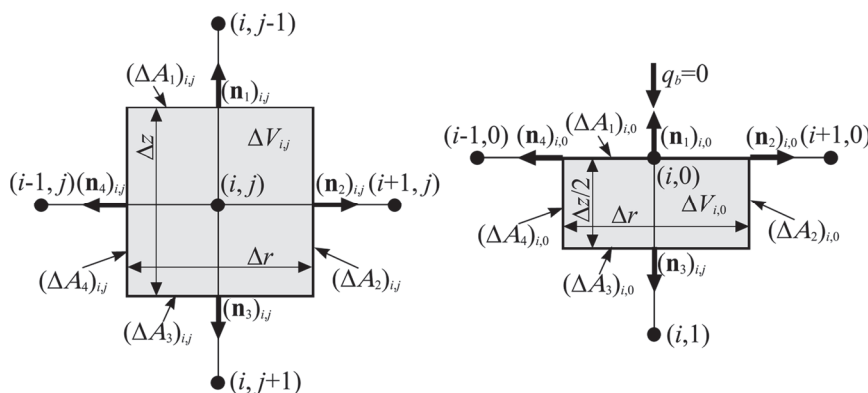


Fig. 3. The internal and boundary control volumes

At the stage of numerical modeling the values of the successive volumes ΔV_{ij} and the values of surfaces limiting ΔV_{ij} must be known, and they can be found on the basis of the simple geometrical considerations.

So, the energy equation (7) should be integrated over the control volume Ω_{ij}

$$\begin{aligned} & \int_{\Omega_{ij}} c \left(\frac{\partial T(r, z, t)}{\partial t} + \tau_q \frac{\partial^2 T(r, z, t)}{\partial t^2} \right) d\Omega \\ & = \int_{\Omega_{ij}} \left(\nabla \cdot [\lambda \nabla T(r, z, t)] + \tau_T \frac{\partial \nabla \cdot [\lambda \nabla T(r, z, t)]}{\partial t} \right) d\Omega \\ & + \int_{\Omega_{ij}} \left(Q(r, z, t) + \tau_q \frac{\partial Q(r, z, t)}{\partial t} \right) d\Omega \end{aligned} \quad (15)$$

The numerical approximation of the left-hand side of equation (7) can be accepted in the form

$$\begin{aligned} & \int_{\Omega_{ij}} c \left(\frac{\partial T(r, z, t)}{\partial t} + \tau_q \frac{\partial^2 T(r, z, t)}{\partial t^2} \right) d\Omega \\ & \cong c_{ij} \left(\frac{\partial T(r, z, t)}{\partial t} \Big|_{r=r_i, z=z_j} + \tau_q \frac{\partial^2 T(r, z, t)}{\partial t^2} \Big|_{r=r_i, z=z_j} \right) \\ & = c_{ij} \left(\frac{dT_{ij}}{dt} + \tau_q \frac{d^2 T_{ij}}{dt^2} \right) \Delta V_{ij} \end{aligned} \quad (16)$$

where $T_{ij} = T(r_i, z_j, t)$, and $c_{ij} = c(T_{ij})$ is an integral mean of thermal capacity in the volume Ω_{ij} . The source term in equation (7) is treated in a similar way



$$\int_{\Omega_{i,j}} \left(Q(r,z,t) + \tau_q \frac{\partial Q(r,z,t)}{\partial t} \right) d\Omega \cong \left(Q_{i,j} + \tau_q \frac{dQ_{i,j}}{dt} \right) \Delta V_{i,j} \quad (17)$$

where $Q_{i,j} = Q(r_i, z_j, t)$.

Applying the divergence theorem to the term determining heat conduction (right hand side of (7)) between the volume $\Omega_{i,j}$ bounded by the surfaces $\Delta A_{i,j}$ and its neighbourhoods one obtains

$$\begin{aligned} & \int_{\Omega_{i,j}} \left(\nabla \cdot [\lambda \nabla T(r,z,t)] + \tau_T \frac{\partial \nabla \cdot [\lambda \nabla T(r,z,t)]}{\partial t} \right) d\Omega \\ &= \int_{\Omega_{i,j}} \nabla \cdot \lambda \left(\nabla T(r,z,t) + \tau_T \frac{\partial \nabla T(r,z,t)}{\partial t} \right) d\Omega \\ &= \int_{A_{i,j}} \left(\mathbf{n} \cdot \lambda \left(\nabla T(r,z,t) + \tau_T \frac{\partial \nabla T(r,z,t)}{\partial t} \right) \right) dA \end{aligned} \quad (18)$$

and next this term can be written in the form

$$\begin{aligned} & \int_{A_{i,j}} \left(\mathbf{n} \cdot \lambda \left(\nabla T(r,z,t) + \tau_T \frac{\partial \nabla T(r,z,t)}{\partial t} \right) \right) dA \\ &= \sum_{k=1}^4 \int_{(\Delta A_k)_{i,j}} \left((\mathbf{n}_k)_{i,j} \cdot (\lambda_k)_{i,j} \left(\nabla T(r,z,t)|_k + \tau_T \frac{\partial \nabla T(r,z,t)}{\partial t}|_k \right) \right) dA_k \\ &\cong \sum_{k=1}^4 (\mathbf{n}_k)_{i,j} \cdot (\lambda_k)_{i,j} \left(\nabla T(r,z,t)|_k + \tau_T \frac{\partial \nabla T(r,z,t)}{\partial t}|_k \right) (\Delta A_k)_{i,j} = \sum_{k=1}^4 (q_k)_{i,j} (\Delta A_k)_{i,j} \end{aligned} \quad (19)$$

where $(q_k)_{i,j}$ can be approximated by the following finite differences (including also the cases of the appropriate boundary conditions (13) on the boundary surfaces)

$$(q_1)_{i,j} = \begin{cases} (\lambda_1)_{i,j} \left(\frac{T_{i,j-1} - T_{i,j}}{\Delta z} + \tau_T \frac{d}{dt} \left(\frac{T_{i,j-1} - T_{i,j}}{\Delta z} \right) \right) & \text{if } j > 0 \\ 0 & \text{if } j = 0 \end{cases} \quad (20)$$

$$(q_2)_{i,j} = \begin{cases} (\lambda_2)_{i,j} \left(\frac{T_{i+1,j} - T_{i,j}}{\Delta r} + \tau_T \frac{d}{dt} \left(\frac{T_{i+1,j} - T_{i,j}}{\Delta r} \right) \right) & \text{if } i < n_r \\ 0 & \text{if } i = n_r \end{cases} \quad (21)$$

$$(q_3)_{i,j} = \begin{cases} (\lambda_3)_{i,j} \left(\frac{T_{i,j+1} - T_{i,j}}{\Delta z} + \tau_T \frac{d}{dt} \left(\frac{T_{i,j+1} - T_{i,j}}{\Delta z} \right) \right) & \text{if } j < n_z \\ 0 & \text{if } j = n_z \end{cases} \quad (22)$$

$$(q_4)_{i,j} = \begin{cases} (\lambda_4)_{i,j} \left(\frac{T_{i-1,j} - T_{i,j}}{\Delta r} + \tau_T \frac{d}{dt} \left(\frac{T_{i-1,j} - T_{i,j}}{\Delta r} \right) \right) & \text{if } i > 0 \\ 0 & \text{if } i = 0 \end{cases} \quad (23)$$

and $(\lambda_k)_{i,j}$ are the harmonic mean thermal conductivity between two central points of adjoining control volumes.

After substitution of all discrete terms into equation (16) one obtains

$$\begin{aligned} c_{i,j} \left(\frac{dT_{i,j}}{dt} + \tau_q \frac{d^2 T_{i,j}}{dt^2} \right) \Delta V_{i,j} &= \sum_{k=1}^4 (q_k)_{i,j} (\Delta A_k)_{i,j} + \\ &+ \left(Q_{i,j} + \tau_q \frac{dQ_{i,j}}{dt} \right) \Delta V_{i,j} \end{aligned} \quad (24)$$

The second stage of CVM is the integration of equation (24) with respect to time. The same effect can be obtained introducing the approximation of time derivatives occurring in (24) by the appropriate finite differences. The energy balance written in the convention of ‘explicit’ scheme (for the transition $t^{f-1} \rightarrow t^f$, $f = 2, \dots, F$) takes the form

$$\begin{aligned} c_{i,j}^{f-1} \left(\frac{T_{i,j}^f - T_{i,j}^{f-1}}{\Delta t} + \tau_q \frac{T_{i,j}^f - 2T_{i,j}^{f-1} + T_{i,j}^{f-2}}{(\Delta t)^2} \right) \Delta V_{i,j} &= \\ &+ \sum_{k=1}^4 (q_k)_{i,j}^{f-1} (\Delta A_k)_{i,j} + \left(Q_{i,j}^f + \tau_q \frac{Q_{i,j}^f - Q_{i,j}^{f-1}}{\Delta t} \right) \Delta V_{i,j} \end{aligned} \quad (25)$$

and

$$(q_1)_{i,j}^{f-1} = \begin{cases} (\lambda_1)_{i,j}^{f-1} \left(\frac{T_{i,j-1}^{f-1} - T_{i,j}^{f-1}}{\Delta z} + \tau_T \frac{1}{\Delta z} \left(\frac{T_{i,j-1}^{f-1} - T_{i,j-2}^{f-2}}{\Delta t} - \frac{T_{i,j}^{f-1} - T_{i,j-2}^{f-2}}{\Delta t} \right) \right) & \text{if } j > 0 \\ 0 & \text{if } j = 0 \end{cases} \quad (26)$$

or (after the transformations)



$$(q_1)_{i,j}^{f-1} = \begin{cases} \frac{(\lambda_1)_{i,j}^{f-1}}{\Delta z} \left(-\left(1 + \frac{\tau_T}{\Delta t}\right) T_{i,j}^{f-1} + \frac{\tau_T}{\Delta t} T_{i,j}^{f-2} + \left(1 + \frac{\tau_T}{\Delta t}\right) T_{i,j+1}^{f-1} - \frac{\tau_T}{\Delta t} T_{i,j+1}^{f-2} \right) & \text{if } j > 0 \\ 0 & \text{if } j = 0 \end{cases} \quad (27)$$

In a similar way, one obtains

$$(q_2)_{i,j}^{f-1} = \begin{cases} \frac{(\lambda_2)_{i,j}^{f-1}}{\Delta r} \left(-\left(1 + \frac{\tau_T}{\Delta t}\right) T_{i,j}^{f-1} + \frac{\tau_T}{\Delta t} T_{i,j}^{f-2} + \left(1 + \frac{\tau_T}{\Delta t}\right) T_{i+1,j}^{f-1} - \frac{\tau_T}{\Delta t} T_{i+1,j}^{f-2} \right) & \text{if } i < n_r \\ 0 & \text{if } i = n_r \end{cases} \quad (28)$$

$$(q_3)_{i,j}^{f-1} = \begin{cases} \frac{(\lambda_3)_{i,j}^{f-1}}{\Delta z} \left(-\left(1 + \frac{\tau_T}{\Delta t}\right) T_{i,j}^{f-1} + \frac{\tau_T}{\Delta t} T_{i,j}^{f-2} + \left(1 + \frac{\tau_T}{\Delta t}\right) T_{i,j+1}^{f-1} - \frac{\tau_T}{\Delta t} T_{i,j+1}^{f-2} \right) & \text{if } j < n_z \\ 0 & \text{if } j = n_z \end{cases} \quad (29)$$

$$(q_4)_{i,j}^{f-1} = \begin{cases} \frac{(\lambda_4)_{i,j}^{f-1}}{\Delta r} \left(-\left(1 + \frac{\tau_T}{\Delta t}\right) T_{i,j}^{f-1} + \frac{\tau_T}{\Delta t} T_{i,j}^{f-2} + \left(1 + \frac{\tau_T}{\Delta t}\right) T_{i-1,j}^{f-1} - \frac{\tau_T}{\Delta t} T_{i-1,j}^{f-2} \right) & \text{if } i > 0 \\ 0 & \text{if } i = 0 \end{cases} \quad (30)$$

where

$$\begin{aligned} (\lambda_1)_{i,j}^{f-1} &= \frac{2\lambda_{i,j}^{f-1}\lambda_{i,j-1}^{f-1}}{\lambda_{i,j}^{f-1} + \lambda_{i,j-1}^{f-1}}, \quad (\lambda_2)_{i,j}^{f-1} = \frac{2\lambda_{i,j}^{f-1}\lambda_{i+1,j}^{f-1}}{\lambda_{i,j}^{f-1} + \lambda_{i+1,j}^{f-1}}, \\ (\lambda_3)_{i,j}^{f-1} &= \frac{2\lambda_{i,j}^{f-1}\lambda_{i,j+1}^{f-1}}{\lambda_{i,j}^{f-1} + \lambda_{i,j+1}^{f-1}}, \quad (\lambda_4)_{i,j}^{f-1} = \frac{2\lambda_{i,j}^{f-1}\lambda_{i-1,j}^{f-1}}{\lambda_{i,j}^{f-1} + \lambda_{i-1,j}^{f-1}} \end{aligned} \quad (31)$$

The acceptance of the ‘directional’ thermal conductivities as the harmonic means of the nodal values causes that in the formulas (30) determining heat fluxes q the thermal resistances between the neighbouring nodes appear (Ciesielski & Mochnacki, 2007a). After the transformations, equation (25) can be written in the final form as

$$\begin{aligned} T_{i,j}^f &= \frac{\Delta t + 2\tau_q}{\Delta t + \tau_q} T_{i,j}^{f-1} - \frac{\tau_q}{\Delta t + \tau_q} T_{i,j}^{f-2} + \\ &\quad \frac{(\Delta t)^2}{(\Delta t + \tau_q)c_{i,j}^{f-1}} \sum_{k=1}^4 (q_k)_{i,j}^{f-1} (\Phi_k)_{i,j} \\ &\quad + \frac{\Delta t}{c_{i,j}^{f-1}} \left(Q_{i,j}^f - \frac{\tau_q}{\Delta t + \tau_q} Q_{i,j}^{f-1} \right) \end{aligned} \quad (32)$$

where $(\Phi_k)_{i,j} = (\Delta A_k)_{i,j} / \Delta V_{i,j}$.

On the basis of the initial conditions (14), the following implementations are used $T_{i,j}^0 = T_{i,j}^1 = T_0$.

In order to determine the stability condition of the explicit differential scheme, the coefficient at

$T_{i,j}^{f-1}$ in equation (32) must be positive. Hence, this condition has the following form

$$\begin{aligned} &\frac{\Delta t + 2\tau_q}{\Delta t + \tau_q} + \frac{(\Delta t)^2}{(\Delta t + \tau_q)c_{i,j}^{f-1}} \left(-\left(1 + \frac{\tau_T}{\Delta t}\right) \right) \\ &\left[\frac{(\Phi_1)_{i,j}}{\Delta z} \begin{cases} (\lambda_1)_{i,j}^{f-1} & \text{if } j > 0 \\ 0 & \text{if } j = 0 \end{cases} + \frac{(\Phi_2)_{i,j}}{\Delta r} \begin{cases} (\lambda_2)_{i,j}^{f-1} & \text{if } i < n_r \\ 0 & \text{if } i = n_r \end{cases} \right. \\ &\left. + \frac{(\Phi_3)_{i,j}}{\Delta z} \begin{cases} (\lambda_3)_{i,j}^{f-1} & \text{if } j < n_z \\ 0 & \text{if } j = n_z \end{cases} + \frac{(\Phi_4)_{i,j}}{\Delta r} \begin{cases} (\lambda_4)_{i,j}^{f-1} & \text{if } i > 0 \\ 0 & \text{if } i = 0 \end{cases} \right] \geq 0 \end{aligned} \quad (33)$$

for each node (i,j) at every moment of time t^f , or in this form

$$\Delta t + 2\tau_q - \Delta t(\Delta t + \tau_T)W_{i,j}^{f-1} \geq 0 \quad (34)$$

where

$$\begin{aligned} W_{i,j}^{f-1} &= \frac{1}{c_{i,j}^{f-1}} \left[\frac{(\Phi_1)_{i,j}}{\Delta z} \begin{cases} (\lambda_1)_{i,j}^{f-1} & \text{if } j > 0 \\ 0 & \text{if } j = 0 \end{cases} + \frac{(\Phi_2)_{i,j}}{\Delta r} \begin{cases} (\lambda_2)_{i,j}^{f-1} & \text{if } i < n_r \\ 0 & \text{if } i = n_r \end{cases} \right. \\ &\quad \left. + \frac{(\Phi_3)_{i,j}}{\Delta z} \begin{cases} (\lambda_3)_{i,j}^{f-1} & \text{if } j < n_z \\ 0 & \text{if } j = n_z \end{cases} + \frac{(\Phi_4)_{i,j}}{\Delta r} \begin{cases} (\lambda_4)_{i,j}^{f-1} & \text{if } i > 0 \\ 0 & \text{if } i = 0 \end{cases} \right] \end{aligned} \quad (35)$$

From inequality (34) one can determine the proper time step Δt

$$\Delta t \in \left[0, \frac{1 + \sqrt{(\tau_T W_{\max} - 1)^2 + 8\tau_q W_{\max}}}{2W_{\max}} - \frac{\tau_T}{2} \right] \quad (36)$$

where $W_{\max} = \max_{(i,j), f} (W_{i,j}^{f-1})$.

4. RESULTS

4.1. The direct problem solution

Numerical simulation of a thermal process subjected to the short-pulse laser heating has been done for the cylindrical domain with dimensions $Z = 100 \cdot 10^{-9}$ [m], $R = 100 \cdot 10^{-9}$ [m]. Thermophysical parameters of material (chromium) are equal to $\lambda = 93$ [W/(mK)], $c = 3.2148 \cdot 10^6$ [J/(m³K)], $\tau_q = 0.136 \cdot 10^{-12}$ [s], $\tau_T = 7.86 \cdot 10^{-12}$ [s] (Tang & Araki, 1999). The parameters of the Gaussian laser pulse are following: $r_d = 50 \cdot 10^{-9}$ [m], $I_0 = 13.7$ [W/m²], $R_f = 0.93$, $\delta = 15.3 \cdot 10^{-12}$ [m], $t_p = 100 \cdot 10^{-15}$ [s]. The initial temperature of the metal is $T_0 = 20$ [°C]. The mesh steps used in this example: $\Delta z = 10^{-9}$ [m], $\Delta r = 10^{-9}$ [m] and the time step $\Delta t = 10^{-16}$ [s].



In figure 4 the temperature histories at the selected points of the domain are shown. Also in this figure the course of the average temperature T_{avg} of the whole domain is presented. One can see that the value of T_{avg} increases by $\Delta T = 0.731324$ [°C] after one laser pulse. Figure 5 presents the courses of isotherms for the selected three moments of time: 0.2 [ps], 0.4 [ps] and 2 [ps].

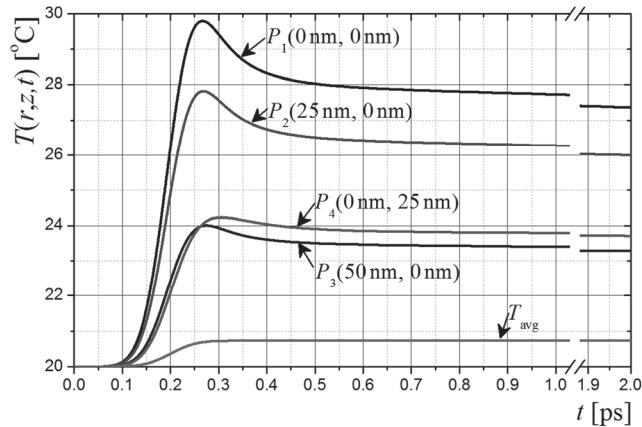


Fig. 4. Heating curves at the selected points and average temperature of domain

4.2. The inverse problem solution

The aim of considerations is the estimation of parameters τ_q and τ_T using the algorithm basing on the search method, at the same time the numerical solution of the task previously discussed is treated as the results of measurements necessary to solve the identification problem.

The search method of the inverse problem solution used here consists in the division of the possible ranges of times $\tau_q \in [\tau_{q\min}, \tau_{q\max}]$ and $\tau_T \in [\tau_{T\min}, \tau_{T\max}]$ into sub-intervals $\Delta\tau_q = (\tau_{q\max} - \tau_{q\min})/n_q$, $\Delta\tau_T = (\tau_{T\max} - \tau_{T\min})/n_T$ and next for each pair $(\tau_q)_i = \tau_{q\min} + i \cdot \Delta\tau_q$ and $(\tau_T)_j = \tau_{T\min} + j \cdot \Delta\tau_T$, for $i = 0, \dots, n_q$ and $j = 0, \dots, n_T$, the direct task is solved. The quality of the solution obtained results from the value of functional J corresponding to least squares criterion

$$J(\tau_q, \tau_T) = \frac{1}{MF} \sum_{m=1}^M \sum_{f=1}^F \left(T_{\tau_q, \tau_T}(r_m, z_m, t_f) - T_d(r_m, z_m, t_f) \right)^2 \quad (37)$$

where M is a number of sensors, F is a number of time steps, T_{τ_q, τ_T} is the calculated temperature

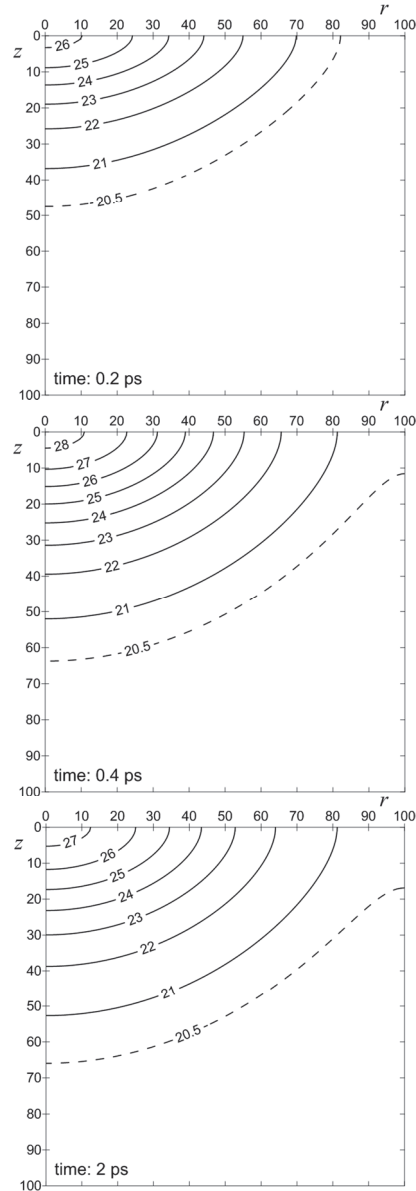


Fig. 5. Courses of isotherms in cross-section of domain for different moments of time

corresponding to assumed values of lag times, T_d is the ‘measured’ temperature. The optimal values of $(\tau_q)_i$ and $(\tau_T)_j$ arises from the minimal value of J .

It was assumed that $T_d(r, z, t)$ is the known temperature at the selected positions of sensors (here: the numerical solution for parameters $\tau_q = 0.136 \cdot 10^{-12}$ [s], $\tau_T = 7.86 \cdot 10^{-12}$ [s]). The possible ranges of times: $\tau_q \in [0.1 \cdot 10^{-12}, 0.2 \cdot 10^{-12}]$ [s], $\tau_T \in [7 \cdot 10^{-12}, 9 \cdot 10^{-12}]$ [s] and the number sensors: $M = 1$ placed at the point ($r = 0, z = 0$) have been taken into account. The calculations were performed for the range of computational time $t \in [0, 10^{-12}]$ [s]. The results are presented in Figure 6.

It should be pointed out that the numerical solution T_d simulating the measurements and the solutions corresponding to T_{τ_q, τ_T} have been obtained



using the different CVM meshes. In accordance with the accepted recommendations for the tasks of this type, the approach proposed assures the more reliable validation of the algorithm concerning the inverse problem solution.

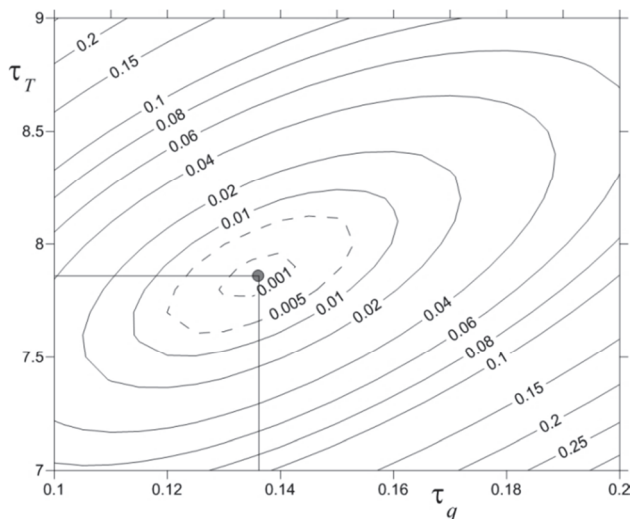


Fig. 6. Solution of inverse problem - values of functional J

5. FINAL REMARKS

The dual phase lag model is being increasingly used for mathematical description of microscale heat transfer. To obtain the effective solution of different problems from this scope the numerical methods must be used, of course. In this paper the algorithm basing on the control volume method is discussed. The version presented allows one to take into account the temperature-dependent thermophysical parameters of material (volumetric specific heat and thermal conductivity) although the example shown in the chapter 4 relates to the constant values of these parameters. The final form of CVM equations is not complicated and simple at the stage of computer program preparation. It is also possible to generalize the basic algorithm by the introduction of numerical procedures simulating the melting, evaporation and finally the ablation of material. In this paper the Neumann boundary condition (laser pulse) is taken into account as an internal heat source. For the strongly scattering material the laser heating is considered in this way, while the irradiated surface is thermally insulated. For highly absorbed materials the

laser heating is approximated as the Neumann boundary condition (Afrin et al., 2012). In such a case the application of the method proposed is also quite simple. The algorithm of the inverse problem solution is very simple one and it requires more computations (solutions of direct tasks) than, for example, the gradient methods (Kurpisz & Nowak, 1995) or evolutionary algorithms (Mochnacki & Paruch, 2013). On the other hand, however, using the approach proposed one obtains the information about the course of functional J in the whole assumed interval of arguments τ_q and τ_T .

ACKNOWLEDGEMENT

The paper is a part of research project 2012/05/B/ST8/01477 sponsored by NSC

REFERENCES

- Afrin, N., Zhou, J., Zhang, Y., Tzou, D.Y., Chen, J.K., 2012, Numerical simulation of thermal damage to living biological tissues induced by laser irradiation based on generalized DPLM, *Numerical heat Transfer, Part A*, 61, 483-501.
- Cattaneo, C., 1958, A form of heat conduction equation which eliminates the paradox of instantaneous propagation, *Comp. Rend.*, 27, 431-433.
- Chen, G., Borca-Tasciuc, D., Yang, R.G., 2004, Nanoscale Heat Transfer, *Encyclopedia of NanoScience and Nanotechnology*, 7, 429-459.
- Chen, J.K., Beraun, J.E., 2001, Numerical study of ultrashort laser pulse interactions with metal films, *Numerical Heat Transfer. Part A*, 40, 1-20.
- Ciesielski, M., Mochnacki, B., 2014a, Application of the control volume method using the Voronoi polygons for numerical modeling of bio-heat transfer processes, *Journal of Theoretical and Applied Mechanics*, 52(4), 927-935.
- Ciesielski, M., Mochnacki, B., 2014b, Numerical simulation of the heating process in the domain of tissue insulated by protective clothing, *Journal of Applied Mathematics and Computational Mechanics*, 13 (2), 13-20.
- Domanski, Z., Ciesielski, M., Mochnacki, B., 2010, Application of Control Volume Method Using the Voronoi Tessellation in Numerical Modelling of Solidification, *Current Themes in Engineering Science 2009*. (ed.) Korsunsky, A., American Institute of Physics, Conf. Proc. 1220, Melville, New York, 17-26.
- Kurpisz K., Nowak A.J., 1995, *Inverse Heat Conduction*, Computational Mechanics Publications Southampton, Boston.
- Majchrzak, E., Mochnacki, B., 2014, Sensitivity analysis of transient temperature field in microdomains with respect to dual-phase-lag model parameters, *International Journal for Multiscale Computational Engineering*, 12 (1), 65-77.
- Majchrzak, E., Mochnacki, B., Greer, A.L., Suchy, J.S., 2009a, Numerical modeling of short pulse laser interactions with multi-layered thin metal films, *CMES – Computer Modeling in Engineering & Sciences*, 41 (2), 131-146.



- Majchrzak, E., Mochnacki, B., Suchy, J.S., 2009b, Numerical simulation of thermal processes proceeding in a multi-layered film subjected to ultrafast laser heating, *Journal of Theoretical and Applied Mechanics*, 47 (2), 383-396.
- Mochnacki, B., Ciesielski, M., 2007a, Application of Thiessen polygons in control volume model of solidification, *Journal of Achievements of Materials and Manufacturing Engineering*, 23 (2), 75-78.
- Mochnacki, B., Ciesielski, M., 2007b, Micro/macro model of solidification. Numerical simulation using the control volume method, *17th International Conference on Computer Methods in Mechanics CMM-2007, CD ROM Proceedings*, 1-4.
- Mochnacki, B., Paruch, M., 2013, Estimation of relaxation and thermalization times in microscale heat transfer, *Journal of Theoretical and Applied Mechanics*, 51 (4), 837-845.
- Szargut, J., 1977, *Numerical methods in thermal computations of industrial furnaces*, Slask, Katowice, (in Polish).
- Tang, D.W., Araki, N., 1999, Wavy, wavelike, diffusive thermal responses of finite rigid slabs to high-speed heating of laser-pulses, *International Journal of Heat and Mass Transfer*, 42, 855-860.
- Tzou, D.Y., 1995, A unified approach for heat conduction from macro- to micro-scale, *ASME Journal of Heat Transfer*, 117, 8-16.
- Zhang, Z.M., 2007, *Nano/microscale heat transfer*, McGraw-Hill, New York.

**PRZEPŁYW CIEPŁA W MIKROSKALI. ALGORYTM
OPARTY NA METODZIE BILANSÓW
ELEMENTARNYCH I IDENTYFIKACJA CZASÓW
RELAKSACJI I TERMALIZACJI ZA POMOCĄ
METODY PRZESZUKIWANIA**

Streszczenie

Procesy cieplne zachodzące w mikro-obszarach mogą być opisane między innymi za pomocą modelu matematycznego z dwoma czasami opóźnień (DPLM). Według najnowszych opinii, model DPLM stanowi bardzo dobry opis rzeczywistych procesów przepływu ciepła w mikroskali, w szczególności ze względu na ekstremalnie krótki czas ich trwania, ekstremalne gradienty temperatury i bardzo małe wymiary geometryczne rozważanego obszaru. Podstawą formułowania DPLM jest uogólnienie prawa Fouriera, w którym występują dwa czasy opóźnień τ_q , τ_T (odpowiednio – czas relaksacji i termalizacji). Numeryczne rozwiązywanie omówionego zagadnienia opiera się na autorskiej wersji Metody Bilansów Elementarnych dostosowanej do rozwiązywania hiperbolicznych równań różniczkowych cząstkowych. Przykład ilustrujący zastosowanie metody dotyczy oszacowania czasów τ_q i τ_T za pomocą algorytmu opartego na metodzie przeszukiwania, oraz rozpatrywana jest cienka folia metalowa poddawana działaniu impulsu laserowego.

*Received: January 23, 2015
Received in a revised form: February 12, 2015
Accepted: March 9, 2015*

